Archives of Acoustics Vol. 49, No. 2, pp. 287–295 (2024), doi: 10.24425/aoa.2024.148783

Technical Note

A Side Lobe Level Reduction Method Using Simulated Annealing Algorithm in a Uniform Arc Array

Song-Il KANG*, Kyong-Sim U, Kyong-Chol CHOE, Yong-Kwang RI, Hyok-Il KYE

Institute of Electronic Materials, High Tech and Development Centre
Kim Il Sung University
Pyongyang, Democratic People's Republic of Korea

*Corresponding Author e-mail: si.kang0604@ryongnamsan.edu.kp

(*received June 22, 2023; accepted January 11, 2024; published online March 19, 2024*)

In general, the amplitude-weighting method for an acoustic transducer array is widely used to improve the array directivity and reject disturbances. This paper presents a method to effectively reduce the side lobe level while minimizing the main lobe width increase. This is done using the simulated annealing algorithm (SAA) for a uniformly spaced arc array of omnidirectional underwater acoustic transducers, even at low signal-to-noise ratio (SNR). We propose a new cost function for the SAA and obtain the weighting coefficients for all array elements using the SAA, and next compare them with various amplitude weighting methods.

Through simulation and comparison, it is verified that the proposed method is effective in beamforming of the uniform arc array of underwater acoustic transducers.

Keywords: underwater acoustic transducer array; beamforming; simulated annealing algorithm; side lobe level reduction.

Copyright © 2024 The Author(s).
This work is licensed under the Creative Commons Attribution 4.0 International CC BY 4.0 (https://creativecommons.org/licenses/by/4.0/).

1. Introduction

Beamforming is used to increase the transmit power and reduce losses in array antennas. Minimizing the side lobe level and enhancing the main lobe level is very important to improve target detection accuracy and jamming stability for underwater acoustic transducer arrays.

For an underwater acoustic transducer array transmitting and receiving a sound wave, a time delay for individual elements steers the acoustic beam in a certain direction, while array amplitude weighting is used to reduce side lobe level, improving the SNR, and jamming suppression capability. Weighting methods of the two-dimensional arrays include the window method (Nofal *et al.*, 2013; Dessouky *et al.*, 2006; 2007; Sarker *et al.*, 2016; Schmerr Jr. 2015; Rucksana Begum, Ramarao, 2015) and various heuristic optimization methods (Albagory, Alraddady, 2021; Singh, Salgotra, 2018; Li *et al.*, 2017; Van Luyen, Vu Bang Giang, 2017). These optimal search weighting methods generally result in optimal position as well as magnitude weight values for array elements if a cylindrical array is used. The window weighting method with the array elements placed at equal spacing suits the requirements of problem we consider in this paper.

Conventional weighting methods effectively reduce the side lobe level. However, it is inevitable that a decrease in the level of the side lobe is accompanied by an increase in the main lobe width. So, we cannot reduce the side lobe level indefinitely, and we must also pay due attention to the degradation of the system resolution due to the widening of the main lobe.

Originally, designed for the annealing heat process in metals, the simulated annealing algorithm (SAA) is now applied to optimal designs. The SAA seeks the solution that minimizes the value of a cost function among a number of possible solutions, which is analogous to the process of finding a stable state with the lowest free energy during annealing. There exist many examples of the SAA used in various optimization problems (Zangene *et al.*, 2014; Chen *et al.*, 2019; Hong *et al.*, 1991; Cretu *et al.*, 2010; Rasdi Rere *et al.*, 2015; Gintaras *et al.*, 2019; Cardone *et al.*, 2002). For instance, Zangene *et al.* (2014) reduced the

side lobe level while minimizing the main lobe width increase by applying the SAA to non-uniform circular arrays used in wireless communication. The authors optimized the position of elements placed in the circumference and the element amplitude weight vector to reduce the main lobe level, and demonstrated that the proposed method is more efficient than genetic algorithm and uniform weighting methods. An application of SAA for acoustic sensors can be found in (Chen *et al.*, 2019), where it is used to effectively reduce the sound pressure level in passenger trains. Many previous methods in which the SAA was used to reduce the side lobe level of the array antenna mostly focused on enhancing the beamforming effect in wireless communication systems and adopted the unequally spaced array.

The SAA was rarely used in underwater signal processing and in the case of arrays used for underwater signal processing, in particular, circular arrays and cylindrical arrays, it is difficult for engineers to arrange acoustic elements with non-uniform spacing at any location. This is because the size of the elements becomes very large due to the fact that the sound velocity is five times higher, and the available frequencies are lower in water than in air.

To overcome this drawback and improve the transmitter and receiver directivity in the acoustic sensor array, the SAA is introduced into the beamforming of uniform arc arrays of underwater acoustic transducers. We propose a new cost function for the SAA and use it to obtain the weight coefficients for the array elements. Thus, we reduce the side lobe level while minimizing the main lobe width increase of the array directivity, even for low signal-to-noise ratio (SNR).

The effectiveness of the proposed method is verified by comparing it with various array weighting methods, such as the cosine weighting method, Hanning weighting method, Hamming weighting method, Blackman weighting method, triangular weighting method, etc. (Schmerr Jr., 2015).

The paper is organized as follows: Sec. 2 briefly describes the array weighting method and the SAA; Sec. 3 presents a new side lobe level reduction method using the SAA; in Sec. 3, the new cost function of SAA and the weighting coefficients of the array elements derived using this SAA are presented; Sec. 4 presents the simulation results, underwater test results, and analysis; Sec. 5 provides the conclusion.

2. Theoretical fundamentals

2.1. Array weighting

Arc arrays are a special case of circular arrays, commonly used in underwater acoustic transducer arrays. The array of interest is a uniform arc array consisting of 12 omnidirectional elements, each positioned with identical central angles between them. An illustration of this arrangement is shown in Fig. 1.

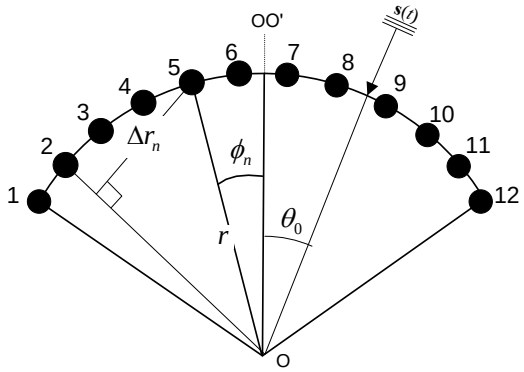

Fig. 1. Uniform arc array with 12 elements.

We assume the signal incident on the array is $\mathbf{s}(t)$, the steering matrix of the array is $\mathbf{A}(\theta, \mathbf{I})$, and the output of the array beamforming is expressed as (Zangene *et al.*, 2014):

$$B(\theta, \mathbf{I}) = |\mathbf{A}(\theta, \mathbf{I})\mathbf{s}(t)|, \tag{1}$$

$$\mathbf{A}(\theta, \mathbf{I}) = [a_1(\theta) \quad a_2(\theta) \quad \cdots \quad a_N(\theta)], \tag{2}$$

$$\mathbf{s}(t) = [s_1(t) \quad s_2(t) \quad \cdots \quad s_N(t)]^{\mathrm{T}}, \tag{3}$$

$$a_n(\theta) = I_n e^{j2\pi f_0 r \cos(\theta - \phi_n)/c}, \quad n = 1, 2, ..., N, \tag{4}$$

$$s_n(t) = A_m e^{j2\pi f_0 (t - t_n)}, \tag{5}$$

$$t_n = r_n/c = r\cos(\theta_0 - \phi_n)/c, \quad n = 1, 2, ..., N, \tag{6}$$

where θ is the angle of interest, $\mathbf{I}$ is the weight vector, I_n is the n-th weight coefficient of the weight vector, f_0 is the center frequency of the signal, θ_0 is the angle of incidence of the signal, r is the radius of the array, c is the propagation velocity of the signal, ϕ_n is the angle from the center line (OO′) to the n-th element, N is the number of elements, and A_m is the signal amplitude. The sign of the angle is positive when its orientation is counterclockwise from the center line and vice versa.

2.2. Simulated annealing algorithm

The SAA yields good results, although it is rather time-consuming. This algorithm, deriving its name from metallurgy, was first proposed by Kirkpatrick *et al.* (1983). The SAA used to improve the directivity of the underwater transducer array minimizes the cost function obtained from the directivity function of the array by setting the initial temperature, final temperature, and the initial weight vector and decreasing the temperature according to certain rules. In subsequent iterations, the weight vector is updated such that the

value of cost function decreases with decreasing temperature. The algorithm prevents the value of the cost function from being trapped in a local minimum and allows it to reach a global minimum. The global minimum is derived by accepting with a certain probability the state in which the cost function increases as well and setting the current state to the state in which the cost function decreases. During the minimization process of cost function, the probability of accepting the state in which the value of the cost function increases gradually drops to zero.

The expression shows the probability of accepting a new state:

$$\mathrm{P}\left(\Delta F(\mathbf{I})\right) = \begin{cases} e^{-\frac{\Delta F(\mathbf{I})}{T}} & \text{if} \quad \Delta F(\mathbf{I}) > 0, \\ 1 & \text{if} \quad \Delta F(\mathbf{I}) \le 0, \end{cases} \tag{7}$$

where $\Delta F(\mathbf{I}) = F_{\text{new}}(\mathbf{I}+\mathbf{I}) - F_{\text{current}}(\mathbf{I})$ is the difference between the cost functions for the new and current states and T is the temperature.

The optimization procedure by the SAA is given as:

1) *Generation of the initial solution vector*: generate the initial vector $\mathbf{I}_0$ and compute the value of the cost function.
2) *Setting of the initial temperature*: in the algorithm, the initial temperature T_0 is very important; if the temperature is too high, the system cannot converge to the minimum state, whereas if it is too low, the global minimum cannot be reached.
3) *Generation of a new solution*: at the temperature T, the new solution $\mathbf{I}_0 + \mathbf{I}$ is generated.
4) *Evaluation of the new solution*: calculate the value of the cost function for the new solution and, based on Eq. (7), accept or reject the new state according to the difference ΔF.
5) *Decrease of the temperature*: decrease the temperature so that the probability of accepting the state in which the value of the cost function increases is reduced.
6) *Repeat of the above steps*: repeat steps 2–5 until the temperature value reaches the final temperature set.

3. The side lobe level reduction method using the SAA

The proposed cost function for reducing the side lobe level to the maximum while minimizing the beam width increase of array directivity is defined as follows:

$$F(\mathbf{W}) = \alpha \left| \frac{W_d - W_I}{W_d} \right| + \beta \frac{\sum_{i=1}^{M} B\left(\theta_{\mathrm{i}}, \mathbf{I}\right)}{B\left(\theta_0, \mathbf{I}\right)}, \tag{8}$$

where θ_i is the position of the i-th side lobe, M is the number of side lobes, $\mathbf{I}$ is the weight vector, W_d is the zero beam width of interest by the weight vector, and W_I is the zero beam width by the weight vector.

While the first term on the right-hand side in Eq. (8) expresses the deviation between the beam width of interest and the beam width by the weight vector, the second term is the ratio of the sum of all the side lobe levels for Eq. (1) to the main lobe level, and the cost function is divided by W_d to be dimensionless.

In Eq. (8), α and β are constants that determine the contributions of the main lobe width and side lobe level, respectively. While the classical cost function (Zangene *et al.*, 2014) considered only the third-order lobe level, the proposed method considers all side lobe levels. Given an array, it is impossible to simultaneously make both the side lobe level and the main lobe width small. Therefore, to optimize the lobe level while minimizing the main lobe width increase, α and β are introduced to reflect the characteristics of the side lobe level and the main lobe width, respectively. Thus, depending on whether the main lobe width or the side lobe level is considered, the values of α and β can be set differently.

In this paper, we theoretically consider the convergence of the proposed cost function for the SAA. The cost function is related to the directivity function of the arc array, which is rather complicated and can only be obtained from numerical calculations. Therefore, we use the approximate equation for the directivity function expressed by the zero-order Bessel function as (Li, 2011):

$$B(\theta) \approx \left| J_0\left(\frac{4\pi r}{\lambda} \sin\left(\frac{\theta - \theta_0}{2}\right)\right)\right|. \tag{9}$$

Equation (9) is satisfied for the uniform arc array under the condition:

$$\frac{1}{\alpha_0} \ge \frac{2r}{\lambda} + \frac{1}{\pi}, \tag{10}$$

where λ is the signal wavelength and α_0 is the central angle between adjacent elements in the radian. Because the cost function is expressed by the Bessel function, as in Eq. (9), the proposed cost function can converge to maintain the main lobe width and simultaneously reduce the side lobe level with changing the weighting coefficients.

Let F_0 be the initial value of cost function, T_0 the initial temperature, T_e the final temperature, $\mathbf{I}_0$ the unit vector, MaxTryT the maximum number of trials at a given temperature, MaxSucT the maximum number of successes at a given temperature, MaxRej the maximum exclusion number, and trialCountT the number of trials at a given temperature. First, we find the difference $\Delta F = F_{\text{new}} - F_{\text{current}}$ between the cost functions for the new and current states by randomly changing the weight vector of the array beamforming output.

The procedure to randomly change the weight vector is as follows:

1) *Generation of random numbers*: generate a random number vector of size $N/2$.
2) *Sorting of random numbers*: sort the generated random number vectors in ascending order.
3) *Symmetrizing of the random number vector*: make a random number vector of size N, symmetrizing the sorted random number vector.
4) *Update of the weight vector*: update the weight vector by adding the random number vector to the current weight vector.
5) *Normalization of the weight vector*: normalize so that the maximum value of the weight vector is equal to 1.

Then, the cost function is updated by introducing the new solution with the transition probability by Eq. (13). This process is repeated while the trial number (trialCountT) is less than the maximum number of trials at a given temperature (MaxTryT) or the success number (sucCountT) is less than the maximum number of successes (MaxSucT) that is to be accepted as a new state. Next, the above process is repeated by changing the temperature in a certain way.

If the temperature reaches the final temperature T_e set or the number of states rejected (countRej) is greater than the maximum rejection number (MaxRej) set, the calculation is ended. The algorithm used in the simulation is shown in Fig. 2.

The solution obtained by the proposed algorithm deviates from the local minima and converges to the global minimum, thus giving good results.

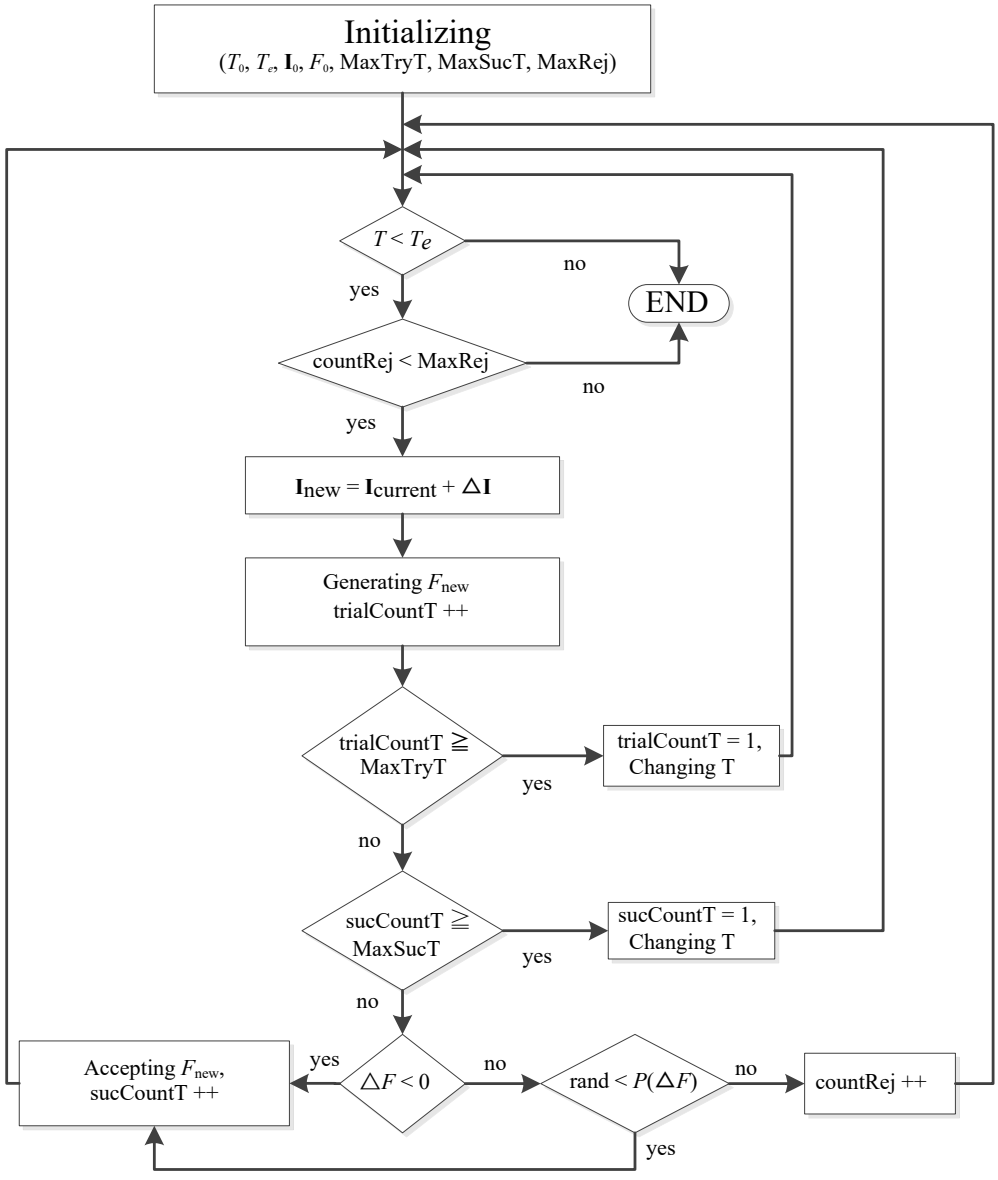

Fig. 2. Computational flow diagram using the proposed algorithm.

4. Simulation and discussion

In the simulation, all the array elements are considered to be omnidirectional. The center angle between each element is 10°, the center frequency of the signal is f_0 = 50 kHz, the speed of sound in water is c = 1500 m/s, and the radius of the arc is r = 0.08 m. For simplicity, let us consider the directivity of the array as the incidence direction of the signal to be set at 0° and the range of angles as [−60°, 60°], while the SNR is varied to −5, 0, 5, 10, 20, and 30 dB.

The initial values of parameters used in the simulation are shown in Table 1.

Figure 3 shows the convergence of the cost function and the temperature throughout the iterative process for the simulation using the proposed method. The temperature drastically reduces until 2000-th iteration and then gradually converges to 0. It can be seen that the convergence process of the cost function exhibits a local minimum around 1445-th iteration, and this is due to the nature of the SAA, which deviates from the local minimum and then converges to the global minimum.

Figure 4 shows the directivity of the arc array obtained by applying various weighting methods and compares them with the proposed method. The side lobe level of the directivity function using the proposed method is −16.6 dB, even for an SNR of −5 dB, but it is about −10 dB for the other methods. It can be seen that the proposed method is effective in side lobe level reduction and powerful over noise suppression, even at low SNRs.

Table 2 presents the weighting factor vectors calculated by the proposed method and the weighting factor values calculated by different methods. Table 3 provides a comparison of different weighting methods with the proposed method for the main lobe width and side lobe level of array directivity at different SNRs. In Table 3, the front values in each column are the 6 dB beam width in degrees, followed by the maximum side lobe levels in dB. From Table 3, it can be seen that at low SNRs below 0 dB, the proposed method minimizes the main lobe width increase, while the side lobe level is the smallest among the seven methods. Furthermore, the main lobe width and the side lobe level do not change significantly at various SNRs. This indicates that the proposed method exhibits high noise robustness.

Table 4 shows the main lobe width (6 dB beam width) and the maximum lobe level of the array directivity with varying values of α and β. From Table 4, it is evident that the main lobe width decreases and the maximum side lobe level increases as β increases.

Figure 5 shows the comparison between the proposed method and various weighting methods using the cost function for different SNRs. Only the maximum side lobe level is used. As shown, the proposed method maintains a constant cost function value, regardless of the SNR change.

Table 1. The initial values of parameters.

Parameters	Initial values
Initial temperature T_0	1
Final temperature T_e	1e-8
Maximum number of trials at a given temperature (MaxTryT)	3000
Maximum Success at a given temperature (MaxScT)	40
Maximum rejection number (MaxRej)	1000
[α, β]	[1, 1]

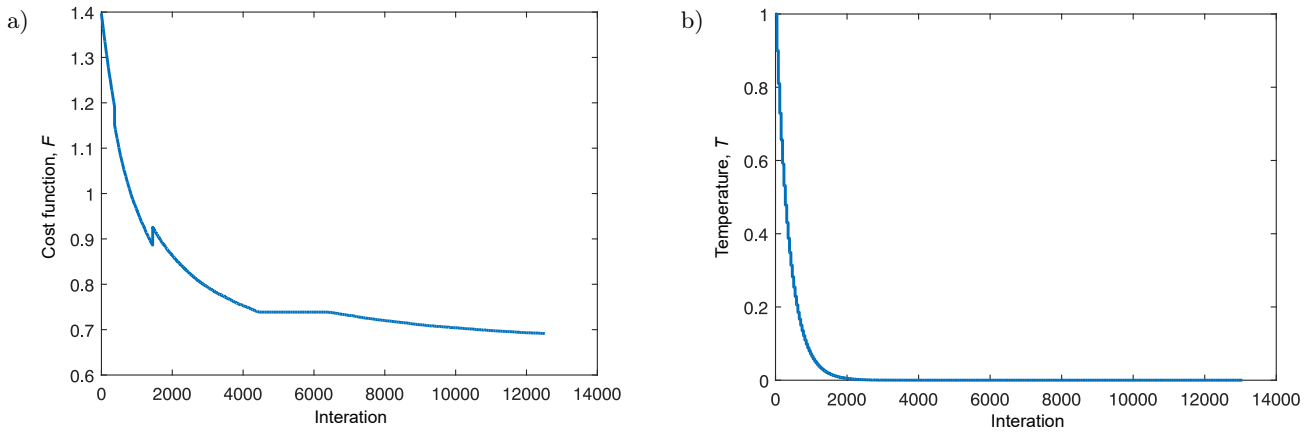

Fig. 3. Convergence of the cost function and the temperature throughout the iterative process: a) convergence; b) temperature.

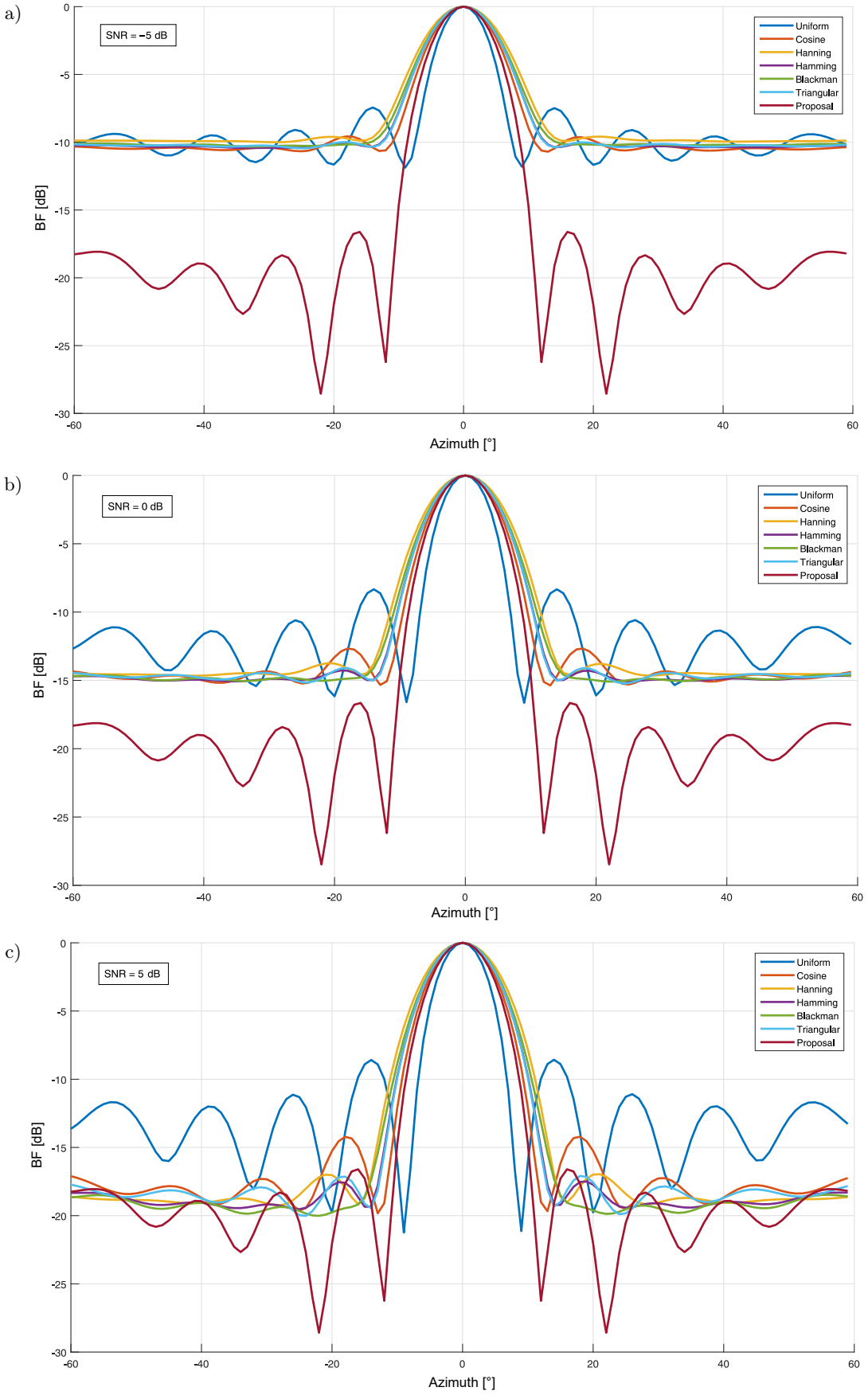
a)
SNR = −5 dB
b)
SNR = 0 dB
c)
SNR = 5 dB
Uniform
Cosine
Hanning
Hamming
Blackman
Triangular
Proposal
BF [dB]
Azimuth [°]

[Fig. 4abc.]

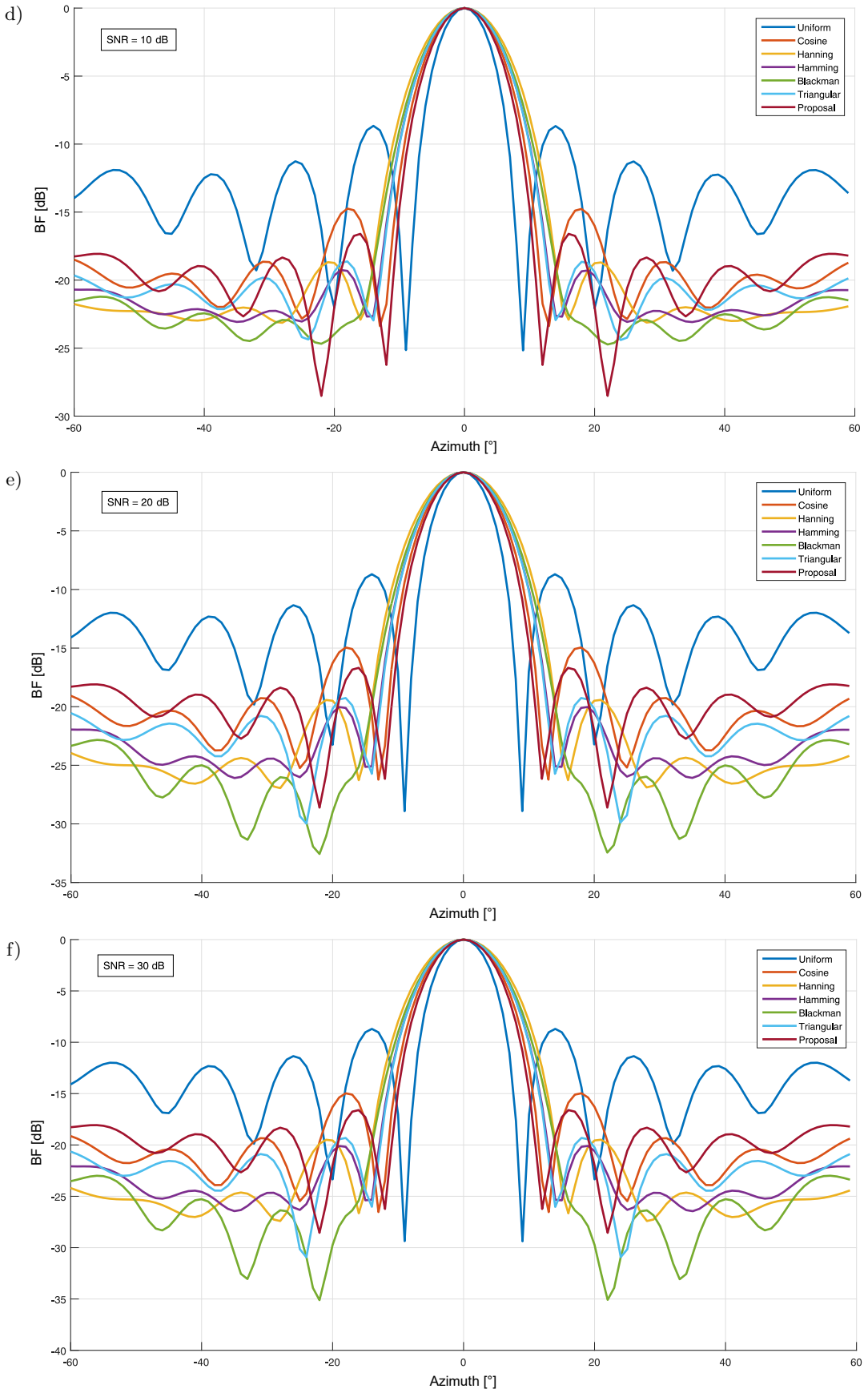

Fig. 4. Comparison between the proposed method and various weighting methodsfor the different SNRs: a) −5 dB; b) 0 dB; c) 5 dB; d) 10 dB; e) 20 dB; f) 30 dB.

Table 2. Weighting vectors by various weighting methods (SNR = 10 dB).

Method	Weighting vector
Uniform	[1, 1, 1, 1, 1, 1, 1, 1, 1, 1, 1, 1]
Cosine	[0, 0.2817, 0.5406, 0.7557, 0.9096, 0.9898, 0.9898, 0.9096, 0.7557, 0.5406, 0.2817, 0]
Hanning	[0.0000, 0.0794, 0.2923, 0.5712, 0.8274, 0.9797, 0.9797, 0.8274, 0.5712, 0.2923 0.0794, 0.0000]
Hamming	[0.0800, 0.1530, 0.3489, 0.6055, 0.8412, 0.9814, 0.9814, 0.8412, 0.6055, 0.3489, 0.1530, 0.0800]
Blackman	[0.1200, 0.1526, 0.2799, 0.5344, 0.8560, 1.0870, 1.0870, 0.8560, 0.5344, 0.2799, 0.1526, 0.1200]
Triangular	[0, 0.1818, 0.3636, 0.5455, 0.7273, 0.9091, 0.9091, 0.7273, 0.5455, 0.3636, 0.1818, 0]
Proposal	[0.2686, 0.4147, 0.5613, 0.7073, 0.8537, 1.0000, 1.0000, 0.8537, 0.7073, 0.5613, 0.4147, 0.2686]

Table 3. Main lobe width and side lobe level for various weighting methods.

Method	SNR [dB]					
	−5	0	5	10	20	30
Uniform	11.6, −7.4	11.4, −8.3	11.2, −8.6	11.2, −8.6	11.0, −8.7	11.0, −8.7
Cosine	16.0, −9.6	15.2, −12.6	15.0, −14.2	14.8, −14.7	14.8, −15.0	14.8, −15.0
Hanning	19.2, −9.6	18.0, −13.7	17.6, −17.0	17.6, −18.6	17.6, −19.4	17.6, −19.5
Hamming	17.2, 10.0	16.6, −14.2	16.4, −17.5	16.2, −19.2	16.0, −20.0	16.0, −20.1
Blackman	18.0, −10.1	17.0, −14.8	16.6, −19.4	16.6, −22.0	16.6, −22.8	16.6, −23.0
Triangular	17.2, −9.9	16.4, −14.1	16.2, −17.1	16.2, −18.6	16.0, −19.2	16.0, −19.3
Proposal	14.0, −16.6	14.0, −16.6	14.0, −16.6	14.0, −16.7	14.0, −16.7	14.0, −16.7

Table 4. Main lobe width and maximum side lobe level for α and β (SNR = 10 dB).

[α, β]	[1,1]	[1,3]	[1,5]	[1,7]	[1,9]
Main lobe width [°]	14.0	13.8	13.6	13.5	13.4
Maximum side lobe level [dB]	−16.7	−16.5	−16.2	−15.9	−15.5

Therefore, it is obvious that the proposed method is effective in improving the directivity pattern of the array and increasing the azimuthal resolution ability by significantly reducing the side lobe level while minimizing the main lobe width increase even for low SNRs.

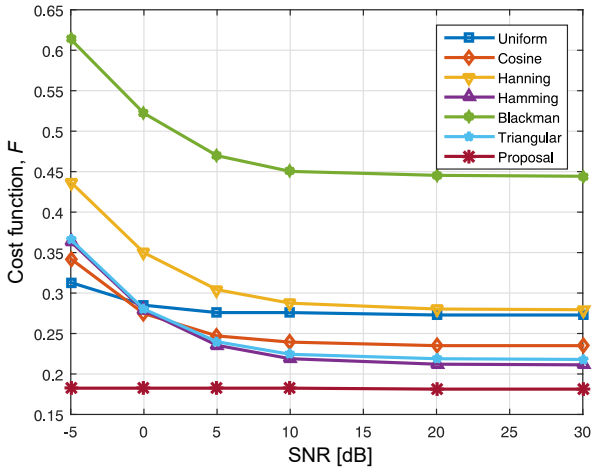

Fig. 5. Comparison of array directivity using the cost function for different SNRs.

5. Conclusion

The array weighting by the proposed method can reduce the side lobe level by about 8 dB lower than the uniform method while minimizing the main lobe width increase for low SNRs. Other methods, except the cosine method, increase the main lobe width considerably, although those may lower the side lobe level more than the proposed method. Therefore, the proposed method can effectively suppress the noise while maintaining the resolution of the underwater acoustic transducer array.

According to the evaluation of directivity by various methods based on the cost function, for the SNR equal to −5 dB, the value of the cost function by the proposed method is 1.55, 1.44, 1.77, 1.39, 2.69, and 1.41 times lower than those by the uniform method, cosine method, Hanning method, Hamming method, Blackman method, and triangular method, respectively.

For uniform arc arrays with underwater acoustic transducers, it is confirmed that array element weighting with weight vectors obtained by using the proposed cost function and simulated annealing based on weight factor updating can effectively reduce the side lobe level while minimizing the main lobe width increase of array directivity even at low SNRs.

References

1. Albagory Y., Alraddady F. (2021), An efficient approach for side lobe level reduction based on recursive sequential damping, *Symmetry*, **13**(3): 480, doi: 10.3390/sym13030480.

2. Cardone G., Cincotti G., Pappalardo M. (2002), Design of wide band arrays for low side-lobe level beam patterns by simulated annealing, [in:] *IEEE Transactions on Ultrasonics, Ferroelectrics, and Frequency Control*, **49**(8): 1050–1059, doi: 10.1109/TUFFC.2002.1026017.
3. Chen W., Gu Z., Ma X., Zhang S., Han Z., Zhong Y. (2019), Robust optimization of vibro-acoustics system based on an elliptical basis function neural network, *Applied Acoustics*, **145**: 41–51, doi: 10.1016/j.apacoust.2018.09.013.
4. Cretu N., Pop M.I., Rosca I.C. (2010), Acoustic design by simulated annealing algorithm, *Physics Procedia*, **3**(1): 489–495, doi: 10.1016/j.phpro.2010.01.064.
5. Dessouky M., Sharshar H., Albagory Y. (2006), Efficient side lobe reduction technique for small-sized concentric circular arrays, *Progress In Electromagnetics Research – PIER*, **65**: 187–200, doi: 10.2528/PIER06092503.
6. Dessouky M., Sharshar H., Albagory Y. (2007), An approach for Dolph-Chebyshev uniform concentric circular arrays, *Journal of Electromagnetic Waves and Applications*, **21**(6): 781–794, doi: 10.1163/156939307780749075.
7. Gintaras P., Tomkevičius A., Ostreika A. (2019), Hybridizing simulated annealing with variable neighborhood search for bipartite graph crossing minimization, *Applied Mathematics and Computation*, **348**: 84–101, doi: 10.1016/j.amc.2018.11.051.
8. Hong G., Zuckermann M., Harris R., Grant M. (1991), A fast algorithm for simulated annealing, *Physica Scripta*, **1991**(T38): 40–44, doi: 10.1088/0031-8949/1991/T38/010.
9. Kirkpatrick S., Gelatt Jr. C.D., Vecchi M.P. (1983), Optimization by simulated annealing, *Science*, **220**(4598): 671–680, doi: 10.1126/science.220.4598.671.
10. Li H., Liu Y., Sun G., Wang A., Liang S. (2017), Beam pattern synthesis based on improved biogeography-based optimization for reducing sidelobe level, *Computers and Electronical Engineering*, **60**: 161–174, doi: 10.1016/j.compeleceng.2017.01.003.
11. Li Q. (2011), *Digital Sonar Design in Underwater Acoustics: Principles and Applications*, pp. 238–242, Zhejiang University Press, Hangzhou.
12. Nofal M., Aljahdali S., Albagory Y. (2013), Tapered beamforming for concentric ring arrays, *AEU – International Journal of Electronics and Communications*, **67**(1): 58–63, doi: 10.1016/j.aeue.2012.06.005.
13. Rasdi Rere L.M., Mohamad I.F., Aniati M.A. (2015), Simulated annealing algorithm for deep learning, *Procedia Computer Science*, **72**: 137–144, doi: 10.1016/j.procs.2015.12.114.
14. Rucksana Begum S., Ramarao G. (2015), Synthesis of non uniform linear arrays using Dolph-Chebyshev polynomial by reducing side lobe level based on modulating parameter array factor, *International Journal of Advance Research in Science and Engineering*, **4**(8): 65–72.
15. Sarker M.A., Hosaain M.S., Masud M.S. (2016), Robust beamforming synthesis technique for low side lobe level using taylor excited antenna array, [in:] *Proceedings of the 2016 2nd International Conference on Electrical, Computer & Telecommunication Engineering*, doi: 10.1109/ICECTE.2016.7879566.
16. Schmerr Jr. L.W. (2015), *Fundamentals of Ultrasonic Phased Arrays*, Springer Cham, pp. 60–65.
17. Singh U., Salgotra R. (2018), Synthesis of linear antenna array using flower pollination algorithm, *Neural Computing & Applications*, **29**: 435–445, doi: 10.1007/s00521-016-2457-7.
18. Van Luyen T., Vu Bang Giang T. (2017), Interference suppression of ULA antennas by phase-only control using bat algorithm, [in:] *IEEE Antennas and Wireless Propagation Letters*, **16**: 3038–3042, doi: 10.1109/LAWP.2017.2759318.
19. Zangene A., Dalili Oskouei H.R., Nourhoseini M. (2014), Reduction of side lobe level in non-uniform circular antenna arrays using the simulated annealing algorithm, *Journal of Electrical and Electronics Engineering Research*, **6**(2): 6–12, doi: 10.5897/JEEER2014.0504.